Computers and Geotechnics 81 (2017) 77–86

Contents lists available at ScienceDirect

Computers and Geotechnics

journal homepage: www.elsevier.com/locate/compgeo

Research Paper

Effect of spatial variability of shear strength on reliability of infinite slopes using analytical approach

Jing-Sen Cai [a], E-Chuan Yan [a], Tian-Chyi Jim Yeh [b,c,*], Yuan-Yuan Zha [d], Yue Liang [e], Shao-Yang Huang [f], Wen-Ke Wang [h], Jet-Chau Wen [f,g]

[a] Faculty of Engineering, China University of Geosciences, Wuhan 430074, China
[b] Tianjin Key Laboratory of Water Resources and Environment, Tianjin Normal University, Tianjin, China
[c] Department of Hydrology and Water Resources, University of Arizona, Tucson, AZ 85721, USA
[d] State Key Laboratory of Water Resources and Hydropower Engineering Science, Wuhan University, Wuhan 430072, China
[e] National Engineering Research Center for Inland Waterway Regulation, Chongqing Jiaotong University, Chongqing 400074, China
[f] Research Center for Soil and Water Resources and Natural Disaster Prevention, National Yunlin University of Science and Technology, Douliou, Taiwan
[g] Graduate School of Engineering Science and Technology, National Yunlin University of Science and Technology, Douliou, Taiwan
[h] Key Laboratory of Subsurface Hydrology and Ecological Effects in Arid Region, Chang'an University, Xi'an, China

ARTICLE INFO

Article history:
Received 18 May 2016
Received in revised form 6 July 2016
Accepted 28 July 2016

Keywords:
Infinite slope
Slope stability
Shear strength
Spatial variability
Analytical approach
Reliability

ABSTRACT

This paper develops an analytical approach for reliability analysis of infinite slope stability in presence of spatially variable shear strength parameters. The analytical approach considers spatial autocorrelation of each parameter and cross-correlations between different parameters. It is robust, computational efficient and provides insight to the importance of spatial correlation scale on slope reliability analysis. This paper also explores the difference in continuous and discrete random fields and emphasizes the importance of fine discretization in relation to correlation scale. Finally, it shows that conditioning the stability analysis with information about trends and spatial data leads to reliability assessments with less uncertainty.

1. Introduction

In slope stability analysis, the criterion that defines the stability is the factor of safety (FS). It is defined as the ratio of the shear strength or resisting force of the slope to the stress or disturbing force. When FS is less than unity, slope failure is assumed to occur. The shear strength of a slope depends on its soil properties. Soil properties such as shear strength parameters and hydraulic conductivity generally exhibit a high degree of spatial variability at various scales (e.g., [1–4]), and it is practically impossible to characterize them in detail within a slope. This reality forces us to cope with uncertain in our evaluations of slope stability. As a consequence, reliability-based analysis is deemed more appropriate than the traditional deterministic approach (e.g., [5,6]).

The spatial variability of shear strength parameters has been shown to play a significant role in reliability analysis of slope stability. For example, Lacasse and Nadim [7] discussed spatial variability and measurement methods in characterizing soil properties in slope stability analysis. They stressed the importance of these uncertainties for geotechnical design. Cho [8] conducted a probabilistic stability evaluation of layered slopes considering spatial variabilities of shear strength parameters and unit weight, and he emphasized the effects of the spatial correlation of soil properties on slope reliability. Griffiths et al. [9] and Jiang et al. [10] indicated that ignoring spatial variability of shear strength parameters could lead to non-conservative estimates (underestimation) of the slope reliability when the coefficients of variation of the shear strength parameters are large. This is particularly important when the factor of safety evaluated using mean values of parameters is close to 1.

It has been well recognized that an infinite slope conceptual model, as a simple model for assessing the factor of safety of shallow landslides or large "length-to-depth ratio" slopes, can yield important insights into slope reliability analyses. For instance,

* Corresponding author at: Tianjin Key Laboratory of Water Resources and Environment, Tianjin University, 393 Binshuixidao Road, Xiqing District, Tianjin 300387, China and Department of Hydrology and Water Resources, The University of Arizona, 1133 E. James E. Rogers Way, 122 Harshbarger Bldg 11, Tucson, AZ 85721, USA.
E-mail address: yeh@hwr.arizona.edu (T.-C.J Yeh).

http://dx.doi.org/10.1016/j.compgeo.2016.07.012
0266-352X/

Griffiths et al. [11] used the infinite slope model to demonstrate effects of spatially variable parameters such as soil strength, slope geometry and pore pressures on the reliability analysis of slope stability. More recently, using this conceptual model, Li et al. [12] illustrated that the linearly increasing mean trend of shear strength parameters has a considerable effect on the reliability analysis of slope stability and critical slip depths. Similarly, Zhang et al. [13] developed a spreadsheet template based on this model for predicting the time-dependent probability of rainfall-induced slope failures. This template enables past performance information to be incorporated, and the uncertainty of different parameters to be considered. Using the infinite slope model, Cho [14] investigated the effect of variation and correlation scale of permeability upon the probability of slope failure and depths of critical slip surfaces during the process of rainfall infiltration. Likewise, with this model, Ali et al. [15] systematically studied the nature of triggering mechanisms and the associated risk of rainfall-induced landslides in the presence of spatially variable hydraulic conductivity.

All these previous studies have relied on Monte Carlo (MC) simulation. That is, the reliability of slope stability analysis is determined based on statistical analysis of factor of safety values derived from a physical model with a large number of generated realizations of parameter values. While MC simulation is a straight-forward approach, it requires a significant amount of computational resources, specifically for multidimensional problems. More importantly, the number of realizations required to obtain a stable estimation is always subjected to questions.

To overcome aforementioned issues associated with MC simulation, this paper develops an analytical approach for reliability analysis of infinite slope stability in presence of spatially variable shear strength parameters. The analytical approach considers spatial autocorrelation of each parameter and cross-correlations between different parameters. Moreover, it allows one to directly relate the spatial statistics of each parameter heterogeneity (mean, variance and correlation scale) through a physical model to the probability of failure, without conducting time-consuming MC simulation.

This article is organized as follows. First, the general procedure of the analytical approach is developed for homogeneous slopes and heterogeneous slopes with either normally or log normally distributed parameters. Subsequently, three illustrative examples of slope reliability analysis (i.e., Infinite undrained clay slope, Infinite clay slope with linearly increasing mean trend and Infinite c'-tanϕ' slope) are investigated to validate the approach. Lastly, implications of the results of these examples for future studies are discussed.

2. Analytical approach of slope reliability

The infinite slope model is a widely accepted model for slope stability analysis in practice (e.g., [11–18]). In particular, shallow landslides with large length-to-depth ratios of the landslide mass, and planar failure surfaces, which are developed parallel to the slope surface, are usually modeled as infinite slopes (Fig. 1(a)), for example, slope failures in the layer of weathered residual soil that overlays the bedrock [14]. Field studies also confirmed that characters of most shallow landslides are consistent with the infinite slope model [12].

Without considering deformation (or neglecting stress-strain relationship), the factor of safety at depth z (FS_z) of an infinite slope (Fig. 1(b)) is often evaluated using the limit equilibrium method (LEM), which can be expressed as follows (e.g., [11,12,14,15]):

$$FS_z = \frac{\tau_f}{\tau_m} = \frac{(z\gamma\cos^2\beta - \sigma^s)\tan\phi' + c'}{z\gamma\sin\beta\cos\beta} = \frac{\tan\phi'}{\tan\beta} + \frac{-\sigma^s\tan\phi' + c'}{z\gamma\sin\beta\cos\beta} \quad (z \leqslant H) \tag{1}$$

where τ_f and τ_m are the shear strength of soil and the shear stress at a given depth z (positive downward), respectively; β is the slope inclination; γ is the total unit weight; H denotes the vertical distance of soils from the slope base to the land surface; σ^s represents the effect of the negative pore water pressure for unsaturated conditions and the positive pore water pressure when saturated at any point of depth z [16]; ϕ' and c' are the effective soil friction angle and the effective cohesion at depth z.

In the following analysis, we will assume that σ^s is zero at all depths within the slope. That is, we assume that there is no presence of water or fluid pressures in the slope. Therefore, Eq. (1) is simplified as:

$$FS_z = \frac{\tan\phi'}{\tan\beta} + \frac{c'}{z\gamma\sin\beta\cos\beta} \quad (z \leqslant H) \tag{2}$$

Because of unknown spatial distribution of the parameter values in Eq. (2), any depth of the slope is a possible "weakest" part within the slope. Hence, a procedure is required to locate the critical slip surface corresponding to the minimum factor of safety. Precisely, the factor of safety (FS) for the entire slope is:

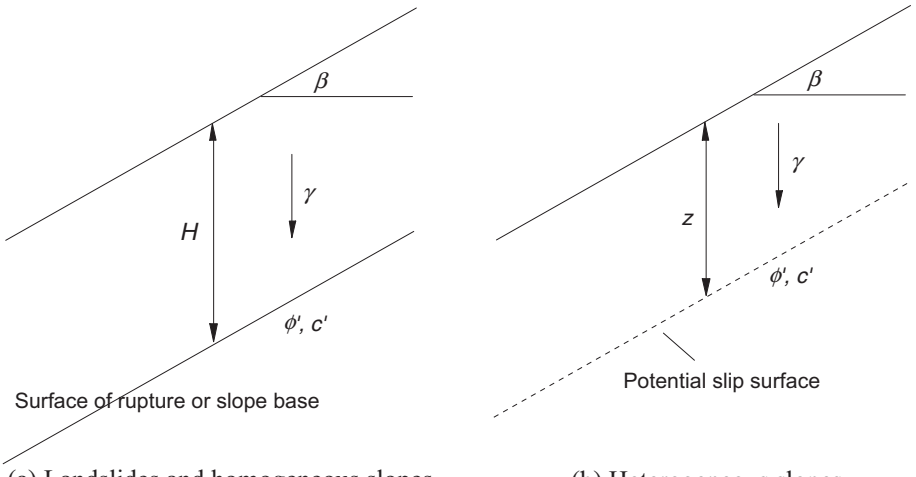

(a) Landslides and homogeneous slopes (b) Heterogeneous slopes

Fig. 1. Infinite slope model.

$$FS = \min\{FS_z\} = \min\left\{\frac{\tan\phi'}{\tan\beta} + \frac{c'}{z\gamma\sin\beta\cos\beta}\right\} \tag{3}$$

Therefore, the probability of failure p_f can be written as follows

$$\begin{aligned} p_f &= 1 - P[\min\{FS_z\} \geqslant 1] \\ &= 1 - P\left[FS_{z_1} \geqslant 1, FS_{z_2} \geqslant 1, \ldots, FS_{z_i} \geqslant 1, \ldots\right] \end{aligned} \tag{4}$$

2.1. Homogeneous slopes

For landslides, there exists a distinct zone of weakness (i.e., surface of rupture) that separates the slide mass from more stable underlying bedrock. For homogeneous slopes, the parameters $\tan\phi'$ and c' are assumed uniform everywhere (spatially invariant), the minimum value of FS_z (i.e., the FS of the entire slope) is obtained at the slope base above the bedrock. Eq. (3) for calculating the factor of safety becomes:

$$FS = \frac{\tan\phi'}{\tan\beta} + \frac{c'}{H\gamma\sin\beta\cos\beta} \tag{5}$$

where the depth z is replaced by H.

The FS in this case is simply the ratio of the shear strength to the shear stress at surface of rupture or slope base (Eq. (5)) without considering deformation [11]. That is to say, the failure probability depends on the values of $\tan\phi'$ and c' at a specific depth H (Fig. 1(a)).

If $\tan\phi'$ and c' at depth H are unknown or undetermined, we have to guess them. As a result, they are best to be considered as random variables, which are described by probability density functions with their means ($\mu_{\tan\phi'}$ and $\mu_{c'}$) and standard deviations ($\sigma_{\tan\phi'}$ and $\sigma_{c'}$). In addition, they may be correlated, and the cross-correlation coefficient between $\tan\phi'$ and c' is then described by $\rho_{\tan\phi' c'}$.

The parameters $\tan\phi'$ and c' are random variables, in turn, FS. As such, FS, $\tan\phi'$ and c' will be expressed in terms of means and perturbations:

$$FS = \mu_{FS} + \Delta FS \quad E[FS] = \mu_{FS} \quad E[\Delta FS] = 0 \tag{6a}$$

$$\tan\phi' = \mu_{\tan\phi'} + \Delta\tan\phi' \quad E[\tan\phi'] = \mu_{\tan\phi'} \quad E[\Delta\tan\phi'] = 0 \tag{6b}$$

$$c' = \mu_{c'} + \Delta c' \quad E[c'] = \mu_{c'} \quad E[\Delta c'] = 0 \tag{6c}$$

Substituting Eq. (6) into Eq. (5), we have

$$\mu_{FS} + \Delta FS = \frac{\mu_{\tan\phi'} + \Delta\tan\phi'}{\tan\beta} + \frac{\mu_{c'} + \Delta c'}{H\gamma\sin\beta\cos\beta} \tag{7}$$

After taking the expected value of this equation, we derive the mean equation for the mean of FS:

$$\mu_{FS} = \frac{\mu_{\tan\phi'}}{\tan\beta} + \frac{\mu_{c'}}{H\gamma\sin\beta\cos\beta} \tag{8}$$

Subtracting mean Eq. (8) from Eq. (7), we then have the equation that relates the perturbation of FS to the perturbations of the parameters.

$$\Delta FS = \frac{\Delta\tan\phi'}{\tan\beta} + \frac{\Delta c'}{H\gamma\sin\beta\cos\beta} \tag{9}$$

After multiplying Eq. (9) with itself, and taking the expectation, we derive the variance of FS:

$$\sigma_{FS}^2 = \frac{\sigma_{\tan\phi'}^2}{\tan^2\beta} + \frac{\sigma_{c'}^2}{(H\gamma\sin\beta\cos\beta)^2} + 2\frac{\sigma_{\tan\phi'}\sigma_{c'}\rho_{\tan\phi' c'}}{H\gamma\sin^2\beta} \tag{10}$$

If we assume $\tan\phi'$ and c' are jointly normally distributed random variables with cross-correlation coefficient $\rho_{\tan\phi' c'}$ (e.g., [11,19]), FS is normal distributed due to the linearity of Eq. (5). Therefore, the probability of failure is given by

$$p_f = P[FS < 1] = \Phi\left[\frac{1 - \mu_{FS}}{\sigma_{FS}}\right] \tag{11}$$

where $\Phi[\cdot]$ is the cumulative standard normal function.

Next, we formulate the probability of failure for the case where the distributions of $\tan\phi'$ and c' are both log-normal. While no sufficient field data have substantiated their log-normal distributions, the log-normal distributions have been widely assumed to avoid negative values of random variable during theoretical analyses (e.g., [11,12,20–25]). Based on this log-normal distribution assumption, Eq. (5) can be rewritten as follows:

$$\ln FS = \ln\left(\frac{e^{\ln\tan\phi'}}{\tan\beta} + \frac{e^{\ln c'}}{H\gamma\sin\beta\cos\beta}\right) \tag{12}$$

where $\ln\tan\phi'$ and $\ln c'$ are treated as random variables. The cross-correlation coefficient between $\ln\tan\phi'$ and $\ln c'$ is then denoted by $\rho_{\ln\tan\phi'\ln c'}$. These random variables can be expressed in terms of their means and perturbations:

$$\ln FS = \mu_{\ln FS} + \Delta\ln FS \quad E[\ln FS] = \mu_{\ln FS} \quad E[\Delta\ln FS] = 0 \tag{13a}$$

$$\ln\tan\phi' = \mu_{\ln\tan\phi'} + \Delta\ln\tan\phi' \quad E[\ln\tan\phi'] = \mu_{\ln\tan\phi'} \quad E[\Delta\ln\tan\phi'] = 0 \tag{13b}$$

$$\ln c' = \mu_{\ln c'} + \Delta\ln c' \quad E[\ln c'] = \mu_{\ln c'} \quad E[\Delta\ln c'] = 0 \tag{13c}$$

Eq. (12) indicates that the relationship between $\ln FS$ and $\ln\tan\phi'$ or $\ln c'$ is nonlinear. In order to linearize the relationship, we use a first order approximation (e.g., [26–29]) based on Taylor series. Then Eq. (12) becomes:

$$\begin{aligned} \mu_{\ln FS} + \Delta\ln FS \approx \ln\left(\frac{e^{\mu_{\ln\tan\phi'}}}{\tan\beta} + \frac{e^{\mu_{\ln c'}}}{H\gamma\sin\beta\cos\beta}\right) \\ + J_{\ln FS\ln\tan\phi'}\Delta\ln\tan\phi' + J_{\ln FS\ln c'}\Delta\ln c' \end{aligned} \tag{14}$$

where $J_{\ln FS\ln\tan\phi'}$ and $J_{\ln FS\ln c'}$ are sensitivities of $\ln FS$ with respect to changes in $\ln\tan\phi'$ and $\ln c'$, respectively. These sensitivities can be evaluated as:

$$J_{\ln FS\ln\tan\phi'} = \left.\frac{\partial\ln FS}{\partial\ln\tan\phi'}\right|_{(\mu_{\ln\tan\phi'},\mu_{\ln c'})} = \frac{1}{1 + e^{(\mu_{\ln c'} - \mu_{\ln\tan\phi'})}/(H\gamma\cos^2\beta)} \tag{15a}$$

$$J_{\ln FS\ln c'} = \left.\frac{\partial\ln FS}{\partial\ln c'}\right|_{(\mu_{\ln\tan\phi'},\mu_{\ln c'})} = \frac{1}{H\gamma\cos^2\beta e^{(\mu_{\ln\tan\phi'} - \mu_{\ln c'})} + 1} \tag{15b}$$

where the vertical bar with subscript implies that the sensitivities are evaluated at the mean values of the shear strength parameters. Therefore, the mean of $\ln FS$ is given by

$$\mu_{\ln FS} \approx \ln\left(\frac{e^{\mu_{\ln\tan\phi'}}}{\tan\beta} + \frac{e^{\mu_{\ln c'}}}{H\gamma\sin\beta\cos\beta}\right) \tag{16a}$$

and the variance is

$$\begin{aligned} \sigma_{\ln FS}^2 \approx J_{\ln FS\ln\tan\phi'}^2\sigma_{\ln\tan\phi'}^2 + J_{\ln FS\ln c'}^2\sigma_{\ln c'}^2 \\ + 2J_{\ln FS\ln\tan\phi'}J_{\ln FS\ln c'}\sigma_{\ln\tan\phi'}\sigma_{\ln c'}\rho_{\ln\tan\phi'\ln c'} \end{aligned} \tag{16b}$$

Because of the linearity of Eq. (14), the probability distribution of $\ln FS$ is normal, and therefore, the probability of failure is given by

$$p_f = P[FS < 1] = P[\ln FS < \ln(1)] \approx \Phi\left[-\frac{\mu_{\ln FS}}{\sigma_{\ln FS}}\right] \tag{17}$$

Again, $\Phi[\cdot]$ is the cumulative standard normal distribution function.

The above detailed derivation for reliability analysis of homogeneous slopes is to elucidate the difference in the analysis of parameter uncertainty in homogeneous slopes and that in heterogeneous

slopes where spatial variabilities of $\tan\phi'$ and c' are considered, as discussed in "Heterogeneous slopes" in the next section. In addition, the result of the analysis is also used to assess the number of realizations required for MC simulation.

2.2. Heterogeneous slopes

Geologic media are inherently heterogeneous at a multiplicity of scales. The homogenous conceptual models discussed above are merely for the sake of convenience in mathematical analysis [2,30]. In order to carry out a more realistic analysis of *FS* for field situations, the analysis must consider the spatial variability of the parameters, $\tan\phi'$ and c'. Because the infinite slope assumption is invoked in this analysis, we will assume that these parameters vary in the vertical direction only (i.e., highly stratified slopes in terms of these two parameters).

Since we do not know exactly the spatial distributions of the two parameters, we treat them as stochastic fields. Each of them is described by a joint probability distribution. In addition to their means and variances, spatial correlation scale, λ, is introduced to represent the distance within which the soil properties (such as $\tan\phi'$ or c') are correlated in space. Physically, the correlation scales describe the average dimensions (e.g., length, thickness) of heterogeneity (e.g., layers, or stratifications) [2].

Because of the heterogeneity and our inability to characterize it, there exist an infinite number of potential slip surfaces (Fig. 1(b)). The problem of evaluating p_f along all the potential slip surfaces is essentially a nondeterministic polynomial-time complete problem [31], which can never be solved exactly [25]. Therefore, p_f is generally estimated using a large but finite number of potential slip surfaces. The rationale of this simplification follows the slope reliability analysis based on MC simulation, in which only finite number of potential slip surfaces are considered for each realization (e.g., [11,12,25,32]). In this study, the total number of potential slip surfaces is denoted as *N*. Note that the intervals between any two neighboring potential slip surfaces are smaller than λ.

Similar to derivation from Eqs. (5)–(10), if the distributions of $\tan\phi'$ and c' at each potential slip surface are assumed to be normal, the mean and auto-covariance of FS_z are given in matrix forms:

$$\boldsymbol{\mu}_{FS_z} = \frac{\mu_{\tan\phi'}}{\tan\beta} + \frac{\mu_{c'}}{\gamma\sin\beta\cos\beta}\frac{1}{\mathbf{z}} \tag{18a}$$

$$\mathbf{R}_{FS_zFS_z} = \frac{\mathbf{R}_{\tan\phi'\tan\phi'}}{\tan^2\beta} + \frac{\mathbf{R}_{c'c'}}{z_iz_j(\gamma\sin\beta\cos\beta)^2} + \frac{\mathbf{R}_{c'\tan\phi'}}{z_i\gamma\sin^2\beta} + \frac{\mathbf{R}_{\tan\phi'c'}}{z_j\gamma\sin^2\beta} \tag{18b}$$

where $i, j = 1, \ldots, N$; $\boldsymbol{\mu}_{FS_z}$ is the $N\times 1$ mean vector for FS_z; $\mathbf{R}_{FS_zFS_z}$, $\mathbf{R}_{\tan\phi'\tan\phi'}$ and $\mathbf{R}_{c'c'}$ are the $N\times N$ auto-covariance matrices for FS_z, $\tan\phi'$ and c', respectively; $\mathbf{R}_{\tan\phi'c'}$ or $\mathbf{R}_{c'\tan\phi'}$ is the $N\times N$ cross-covariance matrix between $\tan\phi'$ and c'. These auto-covariance matrices and cross-covariance matrices could be either generated based on some theoretical models such as Markov function and exponential function (e.g., [11,26,33]) or derived from geostatistical analyses of field data (see [2]). Therefore, the probability of failure is given by

$$\begin{aligned} p_f &= 1 - P[FS_{z_1} \geqslant 1, FS_{z_2} \geqslant 1, \ldots, FS_{z_i} \geqslant 1, \ldots] \\ &\geqslant 1 - P[FS_{z_1} \geqslant 1, FS_{z_2} \geqslant 1, \ldots, FS_{z_N} \geqslant 1] \\ &= 1 - \frac{1}{(2\pi)^{N/2}|\mathbf{R}_{FS_zFS_z}|^{1/2}} \\ &\quad\times \int_1^{+\infty}\cdots\int_1^{+\infty} e^{-\frac{1}{2}(\mathbf{FS_z}-\boldsymbol{\mu}_{FS_z})^T\mathbf{R}^{-1}_{FS_zFS_z}(\mathbf{FS_z}-\boldsymbol{\mu}_{FS_z})} dFS_{z_N}\cdots dFS_{z_1} \end{aligned} \tag{19}$$

where superscript *T* denotes the transpose.

On the other hand, if the distributions of $\tan\phi'$ and c' at each potential slip surface are log-normal, the statistical properties of $\ln FS_z$ are approximated using the first-order analysis based on Taylor series expansion. That is,

$$\boldsymbol{\mu}_{\ln FS_z} \approx \ln\left(\frac{e^{\mu_{\ln\tan\phi'}}}{\tan\beta} + \frac{e^{\mu_{\ln c'}}}{\gamma\sin\beta\cos\beta}\frac{1}{\mathbf{z}}\right) \tag{20a}$$

$$\begin{aligned} \mathbf{R}_{\ln FS_z\ln FS_z} \approx{}& \mathbf{J}_{\ln FS_z\ln\tan\phi'}\mathbf{R}_{\ln\tan\phi'\ln\tan\phi'}\mathbf{J}^T_{\ln FS_z\ln\tan\phi'} \\ &+ \mathbf{J}_{\ln FS_z\ln c'}\mathbf{R}_{\ln c'\ln c'}\mathbf{J}^T_{\ln FS_z\ln c'} \\ &+ \mathbf{J}_{\ln FS_z\ln c'}\mathbf{R}_{\ln c'\ln\tan\phi'}\mathbf{J}^T_{\ln FS_z\ln\tan\phi'} \\ &+ \mathbf{J}_{\ln FS_z\ln\tan\phi'}\mathbf{R}_{\ln\tan\phi'\ln c'}\mathbf{J}^T_{\ln FS_z\ln c'} \end{aligned} \tag{20b}$$

where $\mathbf{J}_{\ln FS_z\ln\tan\phi'}$, $\mathbf{J}_{\ln FS_z\ln c'}$ are $N\times N$ sensitivity diagonal matrices of $\ln FS_z$ with respect to changes in $\ln\tan\phi'$ and $\ln c'$ at different z_i, respectively. Each diagonal entry of $\mathbf{J}_{\ln FS_z\ln\tan\phi'}$ and $\mathbf{J}_{\ln FS_z\ln c'}$ is calculated by:

$$\begin{aligned} J_{\ln FS_z\ln\tan\phi'}(i,i) &= \left.\frac{\partial\ln FS_z(i)}{\partial\ln\tan\phi'(i)}\right|_{(\mu_{\ln\tan\phi'},\mu_{\ln c'})} \\ &= \frac{1}{1+e^{(\mu_{\ln c'}-\mu_{\ln\tan\phi'})}/(z_i\gamma\cos^2\beta)} \end{aligned} \tag{21a}$$

$$J_{\ln FS_z\ln c'}(i,i) = \left.\frac{\partial\ln FS_z(i)}{\partial\ln c'(i)}\right|_{(\mu_{\ln\tan\phi'},\mu_{\ln c'})} = \frac{1}{z_i\gamma\cos^2\beta e^{(\mu_{\ln\tan\phi'}-\mu_{\ln c'})}+1} \tag{21b}$$

where $i = 1, \ldots, N$; $\boldsymbol{\mu}_{\ln FS_z}$ is the $N\times 1$ mean vector for $\ln FS_z$; $\mathbf{R}_{\ln FS_z\ln FS_z}$, $\mathbf{R}_{\ln\tan\phi'\ln\tan\phi'}$ and $\mathbf{R}_{\ln c'\ln c'}$ are the $N\times N$ auto-covariance matrices for $\ln FS_z$, $\ln\tan\phi'$ and $\ln c'$, respectively; $\mathbf{R}_{\ln\tan\phi'\ln c'}$ or $\mathbf{R}_{\ln c'\ln\tan\phi'}$ is the $N\times N$ cross-covariance matrix between $\ln\tan\phi'$ and $\ln c'$. Therefore, the probability of failure is given by

$$\begin{aligned} p_f &= 1 - P[FS_{z_1} \geqslant 1, FS_{z_2} \geqslant 1, \ldots, FS_{z_i} \geqslant 1, \ldots] \\ &\geqslant 1 - P[FS_{z_1} \geqslant 1, FS_{z_2} \geqslant 1, \ldots, FS_{z_N} \geqslant 1] \\ &= 1 - P[\ln FS_{z_1} \geqslant 0, \ln FS_{z_2} \geqslant 0, \ldots, \ln FS_{z_N} \geqslant 0] \\ &= 1 - \frac{1}{(2\pi)^{N/2}|\mathbf{R}_{\ln FS_z\ln FS_z}|^{1/2}} \\ &\quad\times \int_0^{+\infty}\cdots\int_0^{+\infty} e^{-\frac{1}{2}(\ln\mathbf{FS_z}-\boldsymbol{\mu}_{\ln FS_z})^T\mathbf{R}^{-1}_{\ln FS_z\ln FS_z}(\ln\mathbf{FS_z}-\boldsymbol{\mu}_{\ln FS_z})} d\ln FS_{z_N}\cdots d\ln FS_{z_1} \end{aligned} \tag{22}$$

According to Eq. (19) or Eq. (22), the probability of the slope failure will depend on the auto-covariance matrix $\mathbf{R}_{FS_zFS_z}$ or $\mathbf{R}_{\ln FS_z\ln FS_z}$, which is related to spatial correlation scales of the parameters. Physically, this implies that in a slope where parameters are highly correlated in space, if parameters at one location are found to have a value of FS_z greater than 1, the other locations within the correlation scale will likely have a similar value. On the other hand, if the correlation scale is short and the parameters at one location suggest stability of the slope, this information likely cannot be translated to other locations at distances greater than the correlation scale. That is, the probability of failure of a slope thus remains large. This is the physical explanation of effects of the correlation scale on the probability analysis of a slope failure.

It is worth mentioning that there is no closed form for the integration of the multivariate normal distribution in Eqs. (19) and (22). However, there are a number of algorithms that can estimate it numerically [34]. Approximation methods (e.g., MC Methods, Quasi-MC Methods, Polynomial Integration Methods, Subregion Adaptive Methods, Sparse-Grid Methods) are by means of transformation or reparameterization of the original problem and can lead to exact results when given sufficient computational resources. These methods are computationally feasible for moderate accura-

cies and dimensions. Numerical results suggest that typical computation problems require only a few seconds of workstation time [34]. Moreover, these methods are readily available in current software such as MATLAB and R [34]. In this paper, a method based on randomized quasi-random rule is used for integrating the multivariate normal distribution. Further details of the method are given by Genz [35].

3. Examples

In this section, several examples reported in the literature [11,12] are reexamined to assess the above analytical approach.

3.1. Exmaple 1: infinite undrained clay slope

For undrained clay slope, the effective friction angle ϕ' is set to zero, and Eq. (2) can be simplified as

$$\ln FS_z = \ln c' - \ln(z\gamma \sin\beta \cos\beta) \quad (z \leqslant H) \tag{23}$$

In this case, we will consider the spatial variability of the shear strength c' of the undrained slope, and H, γ and β are treated as constants. An example reported by Griffiths et al. [11] is used here, and the following parameters are adopted: $H = 2.5$ m, $\gamma = 20$ kN/m^3 and $\beta = 30°$. 100 potential slip surfaces (i.e., $N = 100$) of different depths at an interval (Δz) of 25 mm are considered. The random field c' is assumed log-normal distributed with $\sigma_{\ln c'} = 0.09975$, $\mu_{\ln c'} = 3.2139$, which is corresponding to $\mu_{c'} = 25$ kN/m^2, $\sigma_{c'} = 2.5$ kN/m^2 in Griffiths et al. [11], and a Markov function is employed for the correlation function:

$$\rho(\Delta z) = \exp[-2\Delta z/\lambda] \tag{24}$$

According to Eqs. (20a) and (20b), the mean and variance of $\ln FS_z$ are given by

$$\boldsymbol{\mu}_{\ln FS_z} = \mu_{\ln c'} - \ln(\mathbf{z}\gamma \sin\beta \cos\beta) \tag{25a}$$

$$\mathbf{R}_{\ln FS_z \ln FS_z} = \mathbf{R}_{\ln c' \ln c'} \tag{25b}$$

The probability of failure, p_f, is then evaluated by Eq. (22).

Fig. 2 shows the comparison of the p_f by the analytical approach and that by MC simulation using 5000 realizations by Griffiths et al. [11], along with the result based on our MC simulation with 160,000 realizations. The realizations of our simulation are generated using the Karhunen-Loeve expansion method (e.g., [15]). This figure demonstrates that the result from analytical approach agrees well with that obtained from MC simulation with 160,000 realizations. This agreement validates the analytical approach. On the other hand, the p_f from Griffiths et al. [11] is slightly smaller than that from analytical approach and the result from our MC simulation. The difference is likely attributed to the fact that 5000 realizations are insufficient to obtain an accurate result.

For the cases with small values of p_f, e.g., $p_f < 0.001$, MC simulation suffers from a lack of efficiency [25]. Our analytical approach is more robust than MC simulation. For example, as β changes to 20° in this example, p_f becomes relatively small, at $\lambda = 1.25$ m or $\lambda/H = 0.5$, p_f is 2.16065×10^{-4} based on the analytical approach. On the other hand, the p_f calculated using MC simulation based on 5000 realizations is quite unstable (i.e., it would change considerably from one evaluation to the next if seed numbers for generating the random field are different). In many cases, the calculated p_f is exactly zero, indicating that the number of realizations below 5000 is insufficient at this low-probability level.

To further demonstrate the effects of the number of realizations on MC results, we use the result from the analytical approach as a reference. Fig. 3 illustrates the p_f by MC simulation and that from the analytical approach for this example as a function of the number of realizations. The result for the case when the slope is homogeneous (correlation scale = infinity) is shown in Fig. 3(a) while Fig. 3(c) displays that for the heterogeneous case where $\lambda = 0.625$ m or $\lambda/H = 0.25$. The results of corresponding cases with normally (rather than long-normally) distributed c' parameters are displayed in Fig. 3(b) and (d), respectively. Fig. 3(a)–(d) all indicate MC simulation requires at least 100,000 realizations to reach a stable and satisfactory result.

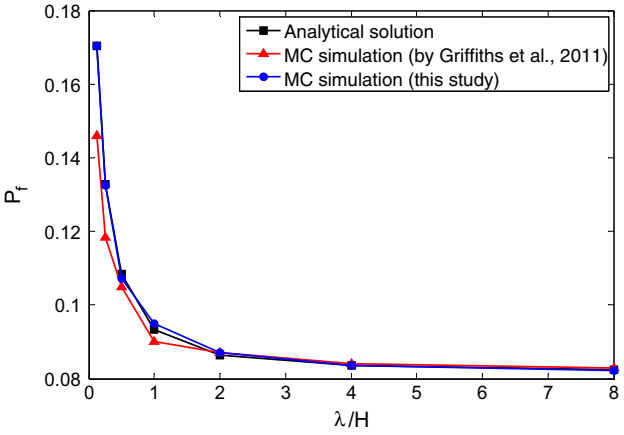

Fig. 2. Comparison of p_f by analytical approach and MC simulation (by Griffiths et al. [11] and by this study) for Example 1 showing the influence of correlation scale.

On the other hand, we also find that the p_f calculated using the analytical approach increases as the number of potential slip surfaces (i.e., N) within the slope increases (see Fig. 4). This increase of p_f value is more significant at small spatial correlation scale to depth ratios (λ/H). In addition, this increase gradually converges to a limit. This finding implies that the p_f is underestimated if N is not sufficiently large, even the analytical approach is used. Such a result may be attributed to discretization associated with the numerical approximation of integration in Eq. (22). However, a similar finding is also reported by Griffiths et al. [11], which employed MC simulation, without the numerical approximation of the integration. We therefore postulate this finding is possibly a result of the difference in continuous stochastic process concept embedded in theories and the discrete stochastic process concept embedded in both MC and the analytical approach. Regardless, in order to avoid this problem, both approximate nature of the numerical integration and our speculated reason suggest that the slope domain should be discretized into a large number of potential slip surfaces. This fine discretization, in effect, may reflect the ensemble REV assumption in all science and engineering as advocated in Yeh et al. [2]. Specifically, in spite of the existence of heterogeneities at any scale, an ensemble REV (or a control volume) is always used to establish a parameter value, which is an ensemble mean (i.e., the average value over all possibilities within the control volume). Finally, it is clear that the interval of potential slip surfaces must be much smaller than a correlation scale length or more potential slip surfaces should be considered within a correlation scale.

3.2. Example 2: infinite clay slope with linearly increasing mean trend

The second example is the case reported by Li et al. [12]. c' is considered to increase linearly with depth and is expressed as $c' = a\gamma' z + b$, where a is considered as a random field. Therefore,

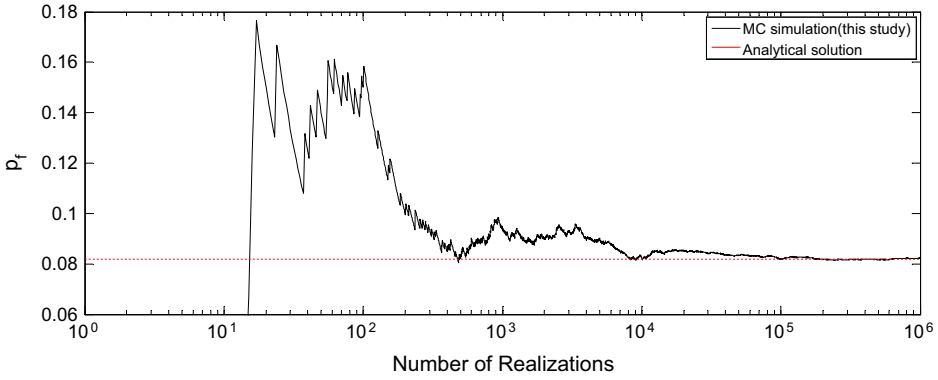

(a) Homogeneous case with log-normally distributed c'

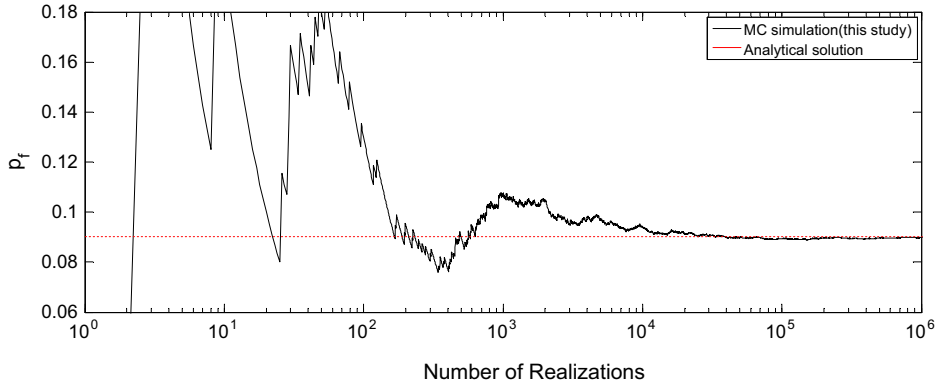

(b) Homogeneous case with normally distributed c'

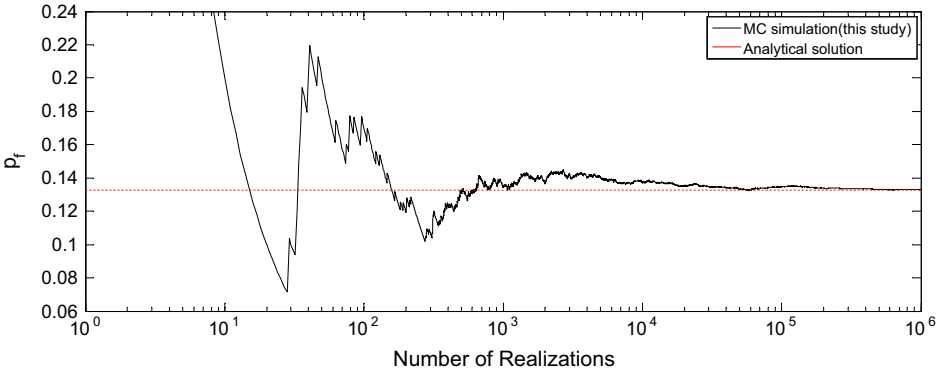

(c) Heterogeneous case ($\lambda/H = 0.25$) with log-normally distributed c'

Fig. 3. Influence of the number of realizations on p_f by MC simulation based on Example 1.

$$FS_z = \frac{a\gamma' z + b}{z\gamma \sin\beta\cos\beta} = \frac{\gamma'}{\gamma \sin\beta\cos\beta}a + \frac{b}{z\gamma \sin\beta\cos\beta} \quad (z \leqslant H) \tag{26}$$

where γ' is the effective unit weight of the soil, a is the rate of change of the undrained shear strength with depth, and b is the value of the undrained shear strength of the soil at the ground surface ($z = 0$).

The following parameters are adopted: $H = 5$ m, $\gamma = 20$ kN/m^3, $\gamma' = 10$ kN/m^3 and $\beta = 30°$. a is log-normal distributed with $\mu_a = 0.8$, $\sigma_a = 0.32$, and 200 potential slip surfaces (i.e., $N = 200$) are considered. Accordingly, p_f is evaluated as follow:

$$\begin{aligned} p_f &= 1 - P\left[FS_{z_1} \geqslant 1, FS_{z_2} \geqslant 1, \ldots, FS_{z_i} \geqslant 1, \ldots\right] \\ &\geqslant 1 - P\left[FS_{z_1} \geqslant 1, FS_{z_2} \geqslant 1, \ldots, FS_{z_{200}} \geqslant 1\right] \\ &= 1 - P\left[\ln\left(\frac{\gamma'}{\gamma \sin\beta\cos\beta}a_{z_i}\right) \geqslant \ln\left(1 - \frac{b}{z_i\gamma \sin\beta\cos\beta}\right), \right. \\ &\qquad \left. i = 1, \ldots, 200\right] \end{aligned} \tag{27}$$

Following Li et al. [12], an exponential autocorrelation function for ln a is used.

$$\rho(\Delta z) = \exp[-\Delta z/\lambda] \tag{28}$$

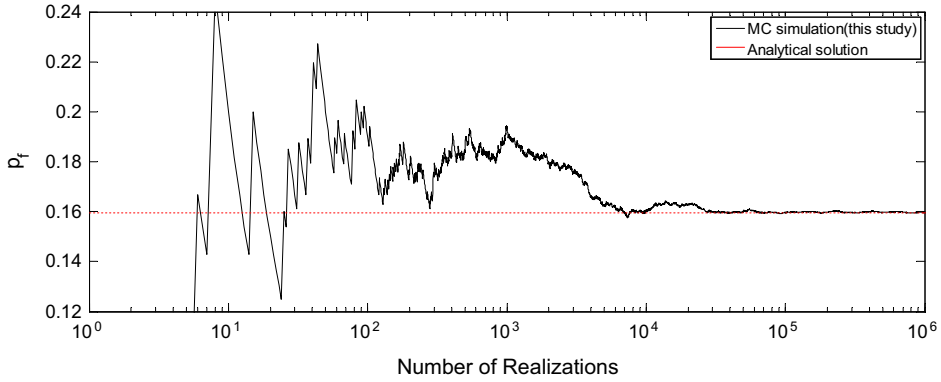

(d) Heterogeneous case ($\lambda/H = 0.25$) with normally distributed c'

Fig. 3 (*continued*)

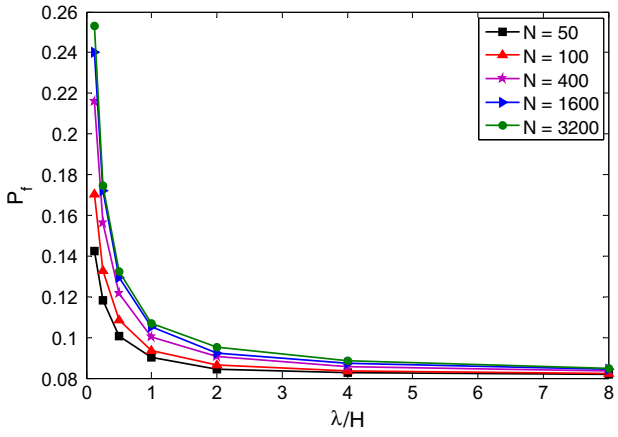

Fig. 4. Effect of the number of potential slip surfaces (N) on p_f at different values of correlation scale based on Example 1.

The comparison of computed p_f by the analytical approach and MC simulation by Li et al. [12] who used more than 10,000 realizations, along with our result based on MC simulation with 100,000 realizations is shown in Fig. 5. These results again agree with each other. Li et al. [12] also compared the result of the linearly increasing trend with that of the case where the trend of c' is ignored. They concluded that the p_f based on the model that considers the linearly increasing trend (i.e., Example 2) is much smaller than that without considering the trend. They emphasized the significance of inclusion of this linear trend information, which leads to a realistic assessment of slope reliability. This is consistent with the ensemble REV concept introduced by Yeh et al. [2,30]. That is, the ensemble REV (the equivalent homogeneous medium) encompasses the variation of large-scale trends in geologic media with multi-scale variability. The variance of the trend is generally greater than the variance of the residuals around the trend. In other words, if the linearly increasing trend of the shear strength is known, its residual variance (uncertainty) will be small and in turn, a more accurate evaluation of p_f is obtained and in this case is reduced.

3.3. Example 3: infinite c'-$\tan\phi'$ slope

The last example for comparison is the one reported by Griffiths et al. [11], where both $\tan\phi'$ and c' are considered spatially variable and they may be correlated. Eq. (2) and Eqs. (18)–(22) are used for this analysis. The following parameters are used: $H = 5$ m, $\gamma = 17$ kN/m^3 and $\beta = 30°$. Both $\tan\phi'$ and c' are treated as random fields with $\mu_{\tan\phi'} = 0.5774$, $\sigma_{\tan\phi'} = 0.17322$, $\mu_{c'} = 10$ kN/m^2 and $\sigma_{c'} = 3$ kN/m^2, respectively. 200 potential slip surfaces (i.e., $N = 200$) are created by discretizing the slope depth into equal parts. A Markov correlation function (Eq. (24)) again is used.

Fig. 6 shows the p_f by the analytical approach and that from our MC simulation with 100,000 realizations assuming that the

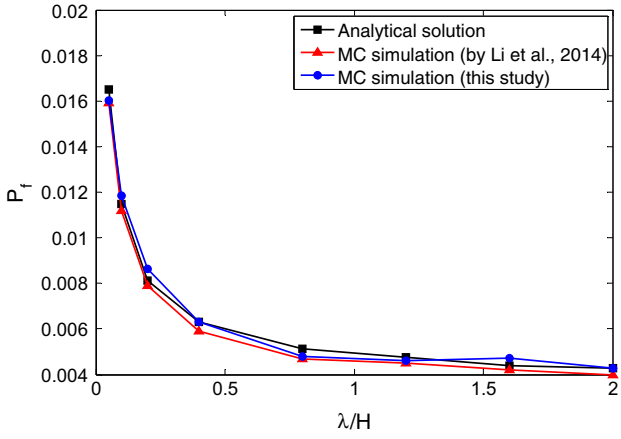

Fig. 5. Comparison of p_f by analytical approach and MC simulation (by Li et al. [12] and by this study) for Example 2, showing the influence of correlation scale.

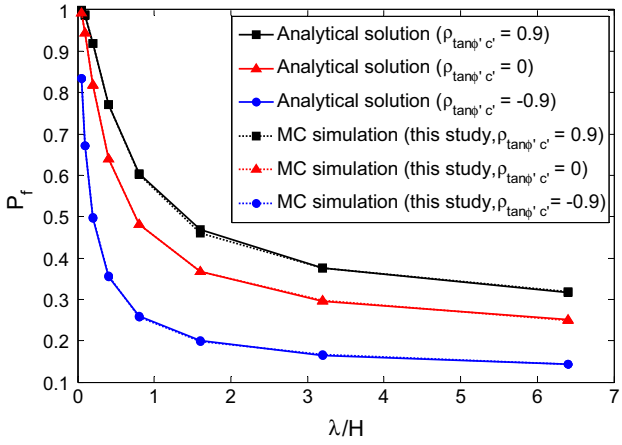

Fig. 6. Comparison of p_f by analytical approach and MC simulation (this study) for Example 3 with normal distributed properties showing the influence of correlation scale and correlation coefficient $\rho_{\tan\phi' c'}$.

distributions of $\tan\phi'$ and c' are normal. The result again validates the proposed approach. Moreover, notice that the p_f increases with the cross-correlation coefficient $\rho_{\tan\phi' c'}$ as expected.

On the other hand, when $\tan\phi'$ and c' are log-normal distributed, FS_z is no longer log-normal or normal distributed. That is, while $\frac{\tan\phi'}{\tan\beta}$ and $\frac{c'}{z\gamma\sin\beta\cos\beta}$ in Eq. (2) are log-normal distributed, their sum does not necessarily possess a log-normal distribution and has no closed-form expression [36]. Several approaches were developed to obtain the distribution of sum of log-normal distributed random variables, such as log-normal approximation or log shifted gamma approximation (e.g., [36–38]), but they are beyond the scope of this study. For practical purpose, a first order approximation based on Taylor series is used here, and the approximated FS_z can be treated as log-normal distributed (i.e., Eqs. (20)–(22)). Based on the approximation, some deviations between the analytical approach and MC simulation are anticipated.

Fig. 7(a) displays the comparison of p_f by the first-order analytical approach, that from MC simulation by Griffiths et al. [11], using 5000 realizations, and that based on our MC simulation with 100,000 realizations. These analyses use $N = 200$ and assume that the distributions of $\tan\phi'$ and c' are log-normal. As indicated in Fig. 7(a), when $\tan\phi'$ and c' are positively correlated or uncorrelated, this first-order analytical approach yields results close to those by both MC simulations. When they are negatively correlated, the analytical approach yields a higher value of p_f than those of the two MC simulations. On the other hand, if they are uncorrelated, the analytical solution is identical to that from our MC simulation.

In Fig. 7(b), we compare the results of the analytical approach and our MC simulation when $N = 2000$. This MC simulation uses 100,000 realizations, the same as our MC simulation in Fig. 7(a). Comparing Fig. 7(a) and (b), the values of p_f evaluated by both MC simulation and analytical approach based on $N = 2000$ are higher than those in Fig. 7(a), where $N = 200$. In addition, the p_f evaluated by our MC simulation and that by the analytical approach are in excellent agreement when the parameters are either uncorrelated or positively correlated. The deviation between the results of our MC simulation and the analytical approach for the negatively correlated case also becomes smaller in comparison with those in Fig. 7(a). These results again suggest the importance of fine discretization of the domain.

The aforementioned results can be explained as follows. If two log-normal distributed random variables (i.e., $\frac{\tan\phi'}{\tan\beta}$ or $\frac{c'}{z\gamma\sin\beta\cos\beta}$) are positively correlated or uncorrelated, extremely small values of them are retained in FS_z when the two distributions are summed up. The resultant distribution of FS_z remains similar to a log-normal distribution (Fig. 8). Therefore, a log-normal distribution approximation works well but it is still an approximation. On the other hand, if these two random variables are negatively correlated, extremely small values of one of the distributions are likely to be lumped into large values of the other, resulting in a distribution like that in Fig. 8, which is similar to exponential distribution or gamma distribution. Hence, the p_f obtained by an approximation using a log-normal distribution deviates from that by MC simulation.

Overall, we have shown that the p_f evaluated by analytical approach agrees well with that by MC simulation when both $\tan\phi'$ and c' are normal distributions. When the log-normal distribution is assumed for $\tan\phi'$ and c', and the coefficients of variations (*CoV*s) of $\tan\phi'$ and c' are small, the approximate analytical approach works well, as log-normal and normal responses are quite similar [11]. Note that Srivastava et al. [39] reported that the general ranges of *CoV*s for ϕ' and c' based on the past studies [3,4,7] are [7,20] for ϕ' and [6,80] for c'. For the case where the *CoV*s of $\tan\phi'$ and c' are large, the p_f produced by the approximate analytical approach may deviate greatly from that by MC simulation. Nevertheless, the relative magnitude trends of the p_f between different events or scenarios are always captured by this approximate analytical approach.

As discussed in Example 2, which considers the spatial trend, conditioning the outcome using more information can reduce uncertainty, and the reliability assessment is more reliable than that based on general models. As a consequence, while values of the *CoV*s of ϕ' and c' reported by Srivastava et al. [39] may be high, the uncertainty due to incomplete knowledge of the heterogeneity of these parameters can be practically reduced if some data are included (i.e., conditional stochastic analysis, see [2,30]). For this reason, the analytical approach, which is capable of conditioning the slope reliability with samples easily, is deem appropriate, and the approximate analytical approach is therefore valid.

We must emphasize that it is virtually impossible to obtain the real distributions of the shear strength parameters in practice. The

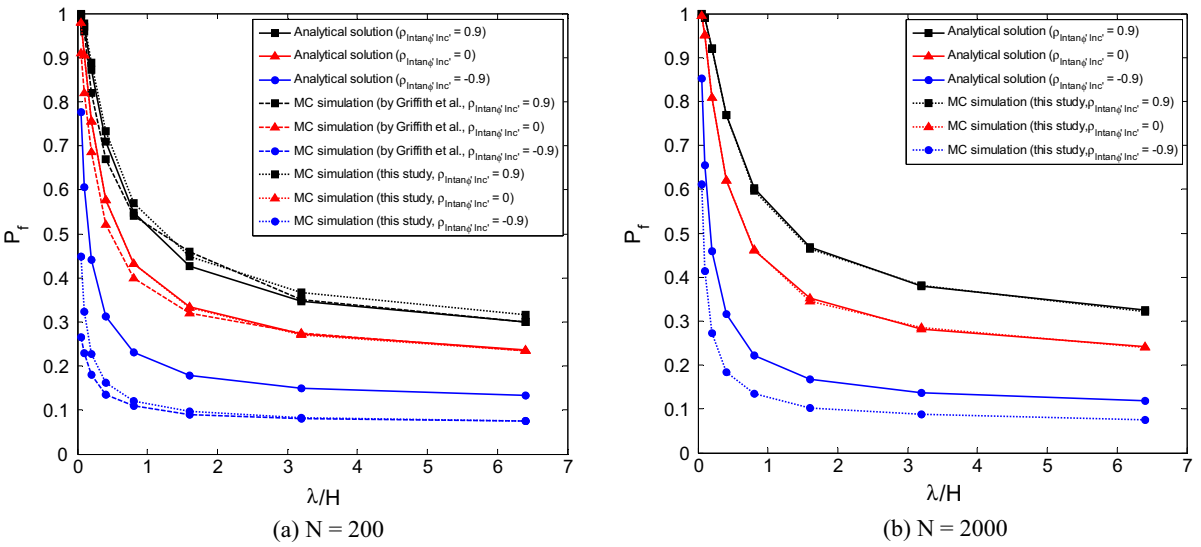

Fig. 7. Comparison of p_f by analytical approach based on first-order approximation and MC simulation (by Griffiths et al. [11] and by this study) for Example 3 with log-normal distributed properties showing the influence of correlation scale and cross-correlation coefficient $\rho_{\ln\tan\phi' \ln c'}$.

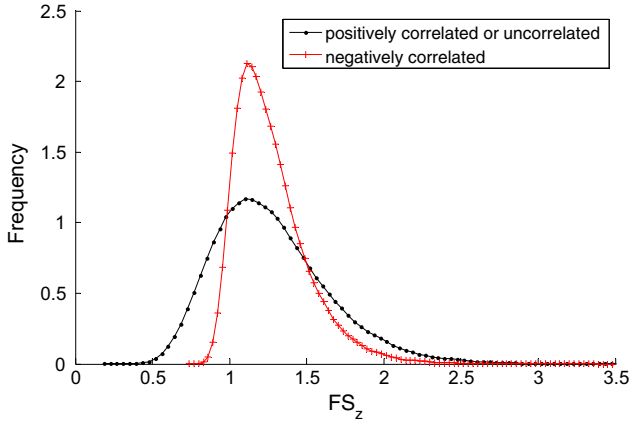

Fig. 8. Illustration for probability density distribution of FS_z when FS_z is the sum of two log-normal distributed random variables.

reported distributions for parameters are merely approximation, unless an infinite number of samples are collected to affirm these distributions. Therefore, if the *CoV*s of the shear strength parameters are large, in spite of the use of any probability distribution models (e.g., normal distribution, log-normal distribution or others), the assessment of slope reliability will yield large uncertainty. In other words, the assessment of slope reliability is inherently a subjective judgment.

At last, we must recognize the fact that the purpose of any reliability analysis aims at evaluation of relative reliability associated with different events or scenarios, rather than the absolute reliability. That is, we are using the estimated value as a criterion to evaluate reliability of different strategies. The fact is that in spite of the accuracy of any theoretic reliability model, result of any reliability analysis (such as MC simulation or analytical approach) is uncertain itself because of uncertainty in input spatial statistics, models, boundaries, initial conditions as well as many other factors. As a consequence, an efficient method such as the analytical approach and first-order analysis is deemed appropriate.

4. Conclusions

The analytical approach for reliability analysis of infinite slope stability is developed and the effect of spatially variable shear strength parameters on reliability of infinite slopes is studied. Three illustrative examples of slope reliability analysis are investigated, and the ability and validity of the developed analytical approach are demonstrated. The following conclusions are drawn from this study:

(1) The analytical approach gives us clear insights into the effects of spatial variability, correlation scales, and cross-correlation of shear strength parameters on p_f.
(2) The interval of potential slip surfaces should be much smaller than a correlation scale length, and this fine discretization is a requirement to avoid underestimating p_f.
(3) The analytical approach provides a means to ensure that MC simulation has sufficient number of realizations such that the p_f evaluated is stable, and further it exhibits greater robustness and higher computational efficiency than MC simulation at small probability levels.
(4) The p_f evaluated by either MC simulation or analytical approaches is dependent on accurate information such as statistics of soil media and geological structures. In order to acquire these pieces of accurate information, intensive spatial and temporal samplings or measurements are required. With these spatiotemporal data, a higher resolution conceptual model with spatially distributed parameters will certainly reduce uncertainty in the evaluation of slope stability. That is, conditional stochastic approaches (e.g., [2,12,30]), which condition the outcome with known and measured parameters, would reduce the uncertainty in the evaluation of slope stability, and lead to a more accurate p_f.

Acknowledgements

This work was supported by the China Scholarship Council (Grant No. 201406410032); the National Natural Science Foundation of China (Grant No. 41172282); the Strategic Environmental Research and Development Program (Grant No. ER-1365); the Environmental Security and Technology Certification Program (Grant No. ER201212); and the National Science Foundation - Division of Earth Sciences (Grant No. 1014594). The third author also acknowledges the Outstanding Oversea Professorship award through Jilin University from Department of Education, China as well as the Global Expert award through Tianjin Normal University from the Thousand Talents Plan of Tianjin City.

Appendix A. Supplementary material

Supplementary data associated with this article can be found, in the online version, at http://dx.doi.org/10.1016/j.compgeo.2016.07.012.

References

[1] Nielsen DR, Biggar JW, Erh KT. Spatial variability of field-measured soil-water properties. University of California, Division of Agricultural Sciences 1973. http://dx.doi.org/10.3733/hilg.v42n07p215.
[2] Yeh T-C, Khaleel R, Carroll KC. Flow through heterogeneous geological media. Cambridge University Press; 2015.
[3] Uzielli M, Lacasse S, Nadim F, Phoon KK. Soil variability analysis for geotechnical practice. In: Proc second int work characterisation eng prop nat soils, Singapore. Netherlands: Balkema; 2006. p. 1653–752.
[4] Duncan JM. Factors of safety and reliability in geotechnical engineering. J Geotech Geoenviron Eng 2000;126:307–16. http://dx.doi.org/10.1061/(ASCE)1090-0241(2000)126:4(307).
[5] Griffiths DV, Fenton GA. Three-dimensional seepage through spatially random soil. J Geotech Geoenviron Eng 1997;123:153–60. http://dx.doi.org/10.1061/(ASCE)1090-0241(1997)123:2(153).
[6] Griffiths DV, Fenton GA. Probabilistic analysis of exit gradients due to steady seepage. J Geotech Geoenviron Eng 1998;124:789–97. http://dx.doi.org/10.1061/(ASCE)1090-0241(1998)124:9(789).
[7] Lacasse S, Nadim F. Uncertainties in characterising soil properties. Publ Geotek Inst 1997;201:49–75.
[8] Cho SE. Effects of spatial variability of soil properties on slope stability. Eng Geol 2007;92:97–109. http://dx.doi.org/10.1016/j.enggeo.2007.03.006.
[9] Griffiths DV, Huang J, Fenton GA. Influence of spatial variability on slope reliability using 2-D random fields. J Geotech Geoenviron Eng 2009;135:1367–78. http://dx.doi.org/10.1061/(ASCE)GT.1943-5606.0000099.
[10] Jiang S-H, Li D-Q, Zhang L-M, Zhou C-B. Slope reliability analysis considering spatially variable shear strength parameters using a non-intrusive stochastic finite element method. Eng Geol 2014;168:120–8. http://dx.doi.org/10.1016/j.enggeo.2013.11.006.
[11] Griffiths DV, Huang J, Fenton GA. Probabilistic infinite slope analysis. Comput Geotech 2011;38:577–84. http://dx.doi.org/10.1016/j.compgeo.2011.03.006.
[12] Li D-Q, Qi X-H, Phoon K-K, Zhang L-M, Zhou C-B. Effect of spatially variable shear strength parameters with linearly increasing mean trend on reliability of infinite slopes. Struct Saf 2014;49:45–55. http://dx.doi.org/10.1016/j.strusafe.2013.08.005.
[13] Zhang J, Huang HW, Zhang LM, Zhu HH, Shi B. Probabilistic prediction of rainfall-induced slope failure using a mechanics-based model. Eng Geol 2014;168:129–40. http://dx.doi.org/10.1016/j.enggeo.2013.11.005.
[14] Cho SE. Probabilistic stability analysis of rainfall-induced landslides considering spatial variability of permeability. Eng Geol 2014;171:11–20. http://dx.doi.org/10.1016/j.enggeo.2013.12.015.
[15] Ali A, Huang J, Lyamin AV, Sloan SW, Griffiths DV, Cassidy MJ, et al. Simplified quantitative risk assessment of rainfall-induced landslides modelled by infinite slopes. Eng Geol 2014;179:102–16. http://dx.doi.org/10.1016/j.enggeo.2014.06.024.

[16] Lu N, Godt J. Infinite slope stability under steady unsaturated seepage conditions. Water Resour Res 2008;44. http://dx.doi.org/10.1029/2008WR006976. n/a–n/a.
[17] Santoso AM, Phoon KK, Quek ST. Effects of soil spatial variability on rainfall-induced landslides. Comput Struct, vol. 89. Elsevier Ltd.; 2011. p. 893–900. http://dx.doi.org/10.1016/j.compstruc.2011.02.016.
[18] Tsai T-L, Tsai P-Y, Yang P-J. Probabilistic modeling of rainfall-induced shallow landslide using a point-estimate method. Environ Earth Sci 2015;73:4109–17. http://dx.doi.org/10.1007/s12665-014-3696-5.
[19] Hicks MA, Samy K. Influence of heterogeneity on undrained clay slope stability. Q J Eng Geol Hydrogeol 2002;35:41–9.
[20] Brejda JJ, Moorman TB, Smith JL, Karlen DL, Allan DL, Dao TH. Distribution and variability of surface soil properties at a regional scale. Soil Sci Soc Am J 2000;64:974. http://dx.doi.org/10.2136/sssaj2000.643974x.
[21] Fenton GA, Griffiths DV. Risk assessment in geotechnical engineering. Wiley; 2008.
[22] Parkin TB, Robinson JA. Analysis of lognormal data. Adv Soil Sci. Springer; 1992. p. 193–235.
[23] Parkin TB, Meisinger JJ, Starr JL, Chester ST, Robinson JA. Evaluation of statistical estimation methods for lognormally distributed variables. Soil Sci Soc Am J 1988;52:323. http://dx.doi.org/10.2136/sssaj1988.03615995005200020004x.
[24] Phoon K-K, Kulhawy FH. Characterization of geotechnical variability. Can Geotech J 1999;36:612–24. http://dx.doi.org/10.1139/t99-038.
[25] Jiang S-H, Li D-Q, Cao Z-J, Zhou C-B, Phoon K-K. Efficient system reliability analysis of slope stability in spatially variable soils using Monte Carlo simulation. J Geotech Geoenviron Eng 2015;141:04014096. http://dx.doi.org/10.1061/(ASCE)GT.1943-5606.0001227.
[26] Cai J, Yan E, Yeh TJ, Zha Y. Effects of heterogeneity distribution on hillslope stability during rainfalls. Water Sci Eng 2016. http://dx.doi.org/10.1016/j.wse.2016.06.004.
[27] Mao D, Yeh TJ, Wan L, Lee C, Hsu K, Wen J, et al. Cross-correlation analysis and information content of observed heads during pumping in unconfined aquifers. Water Resour Res 2013;49:713–31. http://dx.doi.org/10.1002/wrcr.20066.
[28] Mao D, Wan L, Yeh TJ, Lee C, Hsu K, Wen J, et al. A revisit of drawdown behavior during pumping in unconfined aquifers. Water Resour Res 2011;47:W05502. http://dx.doi.org/10.1029/2010WR009326.
[29] Sun R, Yeh TJ, Mao D, Jin M, Lu W, Hao Y. A temporal sampling strategy for hydraulic tomography analysis. Water Resour Res 2013;49:3881–96. http://dx.doi.org/10.1002/wrcr.20337.
[30] Yeh T-C, Mao D, Zha Y, Wen J, Wan L, Hsu K, et al. Uniqueness, scale, and resolution issues in groundwater model parameter identification. Water Sci Eng 2015;8:175–94. http://dx.doi.org/10.1016/j.wse.2015.08.002.
[31] Tang H, Liu X, Xiong C, Wang Z, Ez Eldin MAM. Proof of nondeterministic polynomial-time complete problem for soil slope-stability evaluation. Int J Geomech 2015:C4015004. http://dx.doi.org/10.1061/(ASCE)GM.1943-5622.0000595.
[32] Zhu H, Zhang LM, Zhang LL, Zhou CB. Two-dimensional probabilistic infiltration analysis with a spatially varying permeability function. Comput Geotech 2013;48:249–59. http://dx.doi.org/10.1016/j.compgeo.2012.07.010.
[33] Li D-Q, Jiang S-H, Cao Z-J, Zhou W, Zhou C-B, Zhang L-M. A multiple response-surface method for slope reliability analysis considering spatial variability of soil properties. Eng Geol 2015;187:60–72. http://dx.doi.org/10.1016/j.enggeo.2014.12.003.
[34] Genz A, Bretz F. Computation of multivariate normal and t probabilities, vol. 195. Springer Science & Business Media; 2009.
[35] Genz A. Numerical computation of multivariate normal probabilities. J Comput Graph Stat 1992;1:141–9. http://dx.doi.org/10.1080/10618600.1992.10477010.
[36] Lam CLJ, Le-Ngoc T. Log-shifted gamma approximation to lognormal sum distributions. IEEE Trans Veh Technol 2007;56:2121–9. http://dx.doi.org/10.1109/TVT.2007.897662.
[37] Schwartz SC, Yeh YS. On the distribution function and moments of power sums with log-normal components. Bell Syst Tech J 1982;61:1441–62. http://dx.doi.org/10.1002/j.1538-7305.1982.tb04353.x.
[38] Fenton L. The sum of log-normal probability distributions in scatter transmission systems. IEEE Trans Commun 1960;8:57–67. http://dx.doi.org/10.1109/TCOM.1960.1097606.
[39] Srivastava A, Babu GLS, Haldar S. Influence of spatial variability of permeability property on steady state seepage flow and slope stability analysis. Eng Geol 2010;110:93–101. http://dx.doi.org/10.1016/j.enggeo.2009.11.006.